ISSN 2347-3487
Volume 13 Number 8
Journal of Advance Physics

Structure Analysis, Enhancement of Creep Resistance and Thermal Properties of Eutectic Sn-Ag Lead-Free Solder Alloy by Ti and Cd Additions

B.A.Khalifa, R.Afify Ismail, A.Yassin
Physics department, Faculty of Science, Ain Shams University, Cairo, Egypt.
b.khalifa@sci.asu.edu.eg
Physics department, Faculty of Science, Ain Shams University, Cairo, Egypt.
redaafify@yahoo.com
Physics department, Faculty of Education, Ain Shams University, Cairo, Egypt.
amalyassin477@gmail.com

ABSTRACT

Eutectic (Sn-3.5wt.%Ag) solder alloy is used in electronic circuits in which the creep property of the solder joints is essential for their applications. The study of creep, structure and thermal properties of three solder alloys (Sn-3.5wt.%Ag,Sn-3.5wt.%Ag-0.27wt.%Ti and Sn-3.5wt.Ag-0.27wt.%Cd) is characterized by the presence of (Ag_3Sn-IMC) beside the phase (β-Sn). The microstructure parameters obtained from the X-ray analysis represented by, lattice parameters (a, c), the axial ratio (c/a), the residual strains ($\Delta a/a_0$, $\Delta c/c_0$) and peak height intensities (hkl) of some crystallographic planes are given. All parameters were found to be sensitive to the additions of (Ti or Cd), applied stresses and working temperatures in the range (298-373K).The crystallite size of the (211) reflection was found to increase from (61-132nm) with the additions and to decrease from (115-79nm) with the working temperatures. The morphological studies show a remarkable decrease in the size of (β-Sn) grains with the addition of (Cd) content which confirms the X-ray data. The obtained results show a decrease in melting temperature with the additions. The creep properties are notably improved by the addition of either (Ti) or (Cd). In order to reveal the creep characteristics such as stress exponent (n) and activation energy (Q), the tensile creep tests were performed within the temperature range (298-373K) at constant applied stress (17.27MPa). Based on the obtained stress exponents and activation energies, it is explained that the dominant deformation mechanism is dislocation climb over all temperature range.

Keywords

Lead-free solder alloy, inter metallic compound, microstructure, Ti and Cd-additions, creep properties and thermal properties.

INTRODUCTION

Over the past several decades Pb-Sn systems have been used for conventional solder process owing to combination of material properties and low cost [1-4]. Medical studies have shown that (Pb), the heavy metal toxic can damage kidney, liver, blood and central nervous system [5,6]. In the electronic industry, the (Pb) generated by disposal of electronic assemblies is considered as hazardous environment [7]. Research into the science and engineering of soldering has taken the major change in direction for environment protection in electronic studies [8]. Owing to the consideration of environmental protection and human health, the adoption of Pb-free solder has become an inevitable trend in electronic industry [9]. Therefore rapid switching and great efforts for seeking Pb-free solder alloys with a balance of thermal, mechanical and soldering properties as a replacement for Sn-Pb alloy [10]. SnAg alloys are being considered as one of the most favorable Pb-free solder system. In this respect numerous studies have been devoted to the microstructure of SnAg solder alloys [11-16]. M.L.Huang et.al. have been carried the creep behavior of eutectic Sn-3.5Ag alloy at three different temperatures ranging from (303-393K), and found that (Ag_3Sn IMCs) were finely dispersed in the β-Sn matrix [17]. However, some problems of this alloy still exist due to short creep rupture life time and high cost. In addition the formation of (Ag_3Sn IMCs) in the solder matrix deteriorates the mechanical performance of a solder joint, leading to failure under stress conditions in actual services [18].

Since the properties of the binary Pb-free solders cannot fully meet the requirements for applications in electronic, packaging, additional alloying elements were added to improve the performance of these alloys. Thus, ternary and even quaternary Pb-free solders have been developed [19-23].

To provide an excellent performance improving solder microstructure, reducing IMC growth and increasing the drop life time, the coarse β-Sn grain in the alloy solder become finer and uniform by the addition of trace Ti element [9].

Although cadmium has only limited use as a pure metal it forms binary and more complex alloys which has useful properties for many commercial applications Its presence improve the hardness, wear resistance, mechanical strength, fatigue strength, cast ability and electrochemical properties of a number of alloys [24,25].

In order to understand the thermo mechanical performance for electronic applications for the Sn–Ag solder alloys, the present study was developed to investigate the microstructure and mechanical behavior at (different stresses, temperatures and additions). Correlation between the microstructure and mechanical properties due to Cd or Ti additions were discussed.

DOI : 10.24297/jap.v13i8.6357
www.cirworld.com

1 EXPERIMENTAL PROCEDURE

In the present study the Pb-free solders with the compositions (wt.%) of Sn-3.5Ag (S1), Sn-3.5Ag-0.27Ti (S2) and Sn-3.5Ag-0.27Cd (S3) were prepared from Sn, Ag, Ti and Cd with purity of about 99.99% by melting in a clean graphite crucible. The alloy materials (ingots) were swaged in wire form of (0.7mm) diameter and the gauge length of ($3x10^{-2}$ m). The wire samples were re-annealed at (373K) for 6-hours, then slowly cooled inside a switched off furnace to obtain samples containing the fully precipitated phases and free from any plastic strain accumulation during machining.

Creep test for samples were carried out under different applied stresses in the range of (11.4-25.1MPa) and at different working temperatures (298, 323, 348 and 373 K) which were monitored by a thermocouple contacting with the specimen (within accuracy of ± 1°C).

The structure of the original alloys (S1, S2, and S3) has been studied to identify the effect of the addition (Ti or Cd). The effect of working temperatures ranging from (298-373K) on the alloy (S3) crept at constant applied stress (17.27MPa) were traced through the analysis of the obtained X-ray diffraction (XRD) using Philips X' Pert (MPD) goniometer PW3050/00 with graphite monochromatic using Cu-Kα target and Ni filter operated at (40 K.V.) and (30 mA) to give radiation of wave length (λ = 0.15406 nm).

The morphology of the original alloy samples (S1, S2, S3) were examined by scanning electron microscope (SEM) micrographs. A solution of 2 % HCl, 3% HNO_3 and 95 % (Vol.) Ethyl alcohol was used to make etching of the samples.

In order to understand the thermal behaviors of the three original solder alloys (S1, S2, S3), differential thermal analyses (DTA) were carried out at heating rate of (10 ºC/min.) in nitrogen flow atmosphere.

2 RESULTS AND DISCUSSIONS

2.1 Creep Properties

Figure 1(a,b,c,d) shows typical creep behavior of (S1, S2, S3) solder materials at (17.27MPa) and temperatures (298, 323, 348 and 373K) respectively. Apparently, the shapes of the curves are conventional, with a well defined secondary creep stage II right after loading with a very little primary creep stage I. The tertiary creep deformation characteristic can also be seen clearly at the same stress level and temperatures. The minimum creep rate ε_s was taken at the steady state stage and its variation suggests a basic change in the internal stress. This implies that the hardening of the matrix was recovered immediately and balanced at extended deformation rate [26].

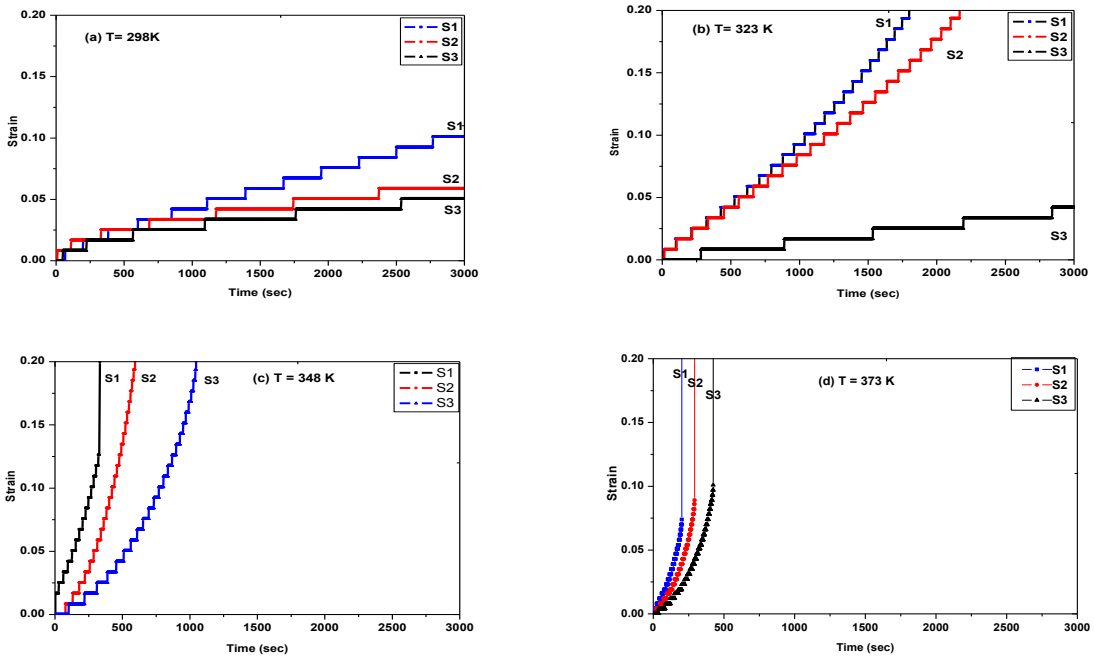

Figure 1(a, b, c, d): Creep behavior of S1,S2 and S3 solder materials at constant applied stress (σ=17.27MPa) and at different working temperatures

Additional information on the dominant deformation mode can be characterized by the corresponding creep rate-time relationship of the selected solder alloys as shown in Figure 1(e). It is typical with the behavior patterns displayed by most metals and alloys [27]. However one can see that the three solders exhibit a well defined, steady state behavior. The decrease in creep rate with time reflects the gradually change from a primary-dominant to tertiary-dominant curve shape with increasing test duration and temperature. The minimum creep rate ε_s is generally reached when the decreasing creep rate is offset by the tertiary acceleration. However with the addition of (Ti or Cd) to S1 solder, the creep properties were enhanced. The effect of working temperature on S2 alloy at constant applied stress (as an example) is shown in Figure 2.

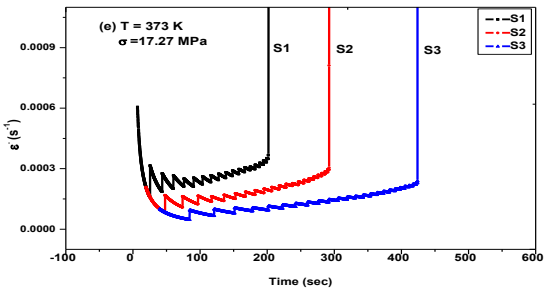

Figure 1(e): Creep rate – time relationship

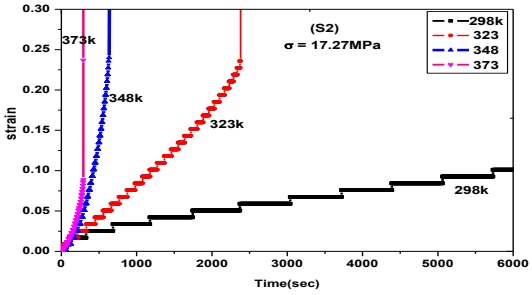

Figure 2: Effect of working temperatures on S2

2.2 Constitutive Creep Equation and Parameters

Previous studies indicated that the dependence of steady state creep rate ε_s on the applied stress (σ) and temperature T can be expressed as

$$\dot{\varepsilon}_s = A\sigma^n \exp(-Q/RT) \quad (1)$$

Where A is a complex constant depends on the material structural properties [28]. Taking the natural logarithm on both sides of equation (1), we get:-

$$\ln \dot{\varepsilon}_s = \ln A + n \ln \sigma - Q/RT \quad (2)$$

It is clear that at a given temperature the creep stress exponent (n) can be calculated by linear regression of the experimental data. It is assumed that the deformation is dominant by one creep mechanism in the whole stress range applied; therefore the stress exponent can be taken as a constant at any given temperature. Figure 3 (a,b,c,d) shows linear relationships between (ln ε_s and ln σ). The relationship between the exponents (n) for the three sample alloys as a function of working temperatures is shown in Figure 3 (e). The relation (ln ε_s and 1/T) is represented in Figure 4. In contrast, the (Q) value of sample (S1) alloy is (37.4KJ/mol.). It is increased to (52.3KJ/mol.) & (57.5KJ/mol.) by the addition of the (Ti) & (Cd) respectively. The creep characteristics (n & Q) are tabulated in Table 1, these values are complied with the reported value of (Sn-Ag) which is controlled by dislocation climb [29].

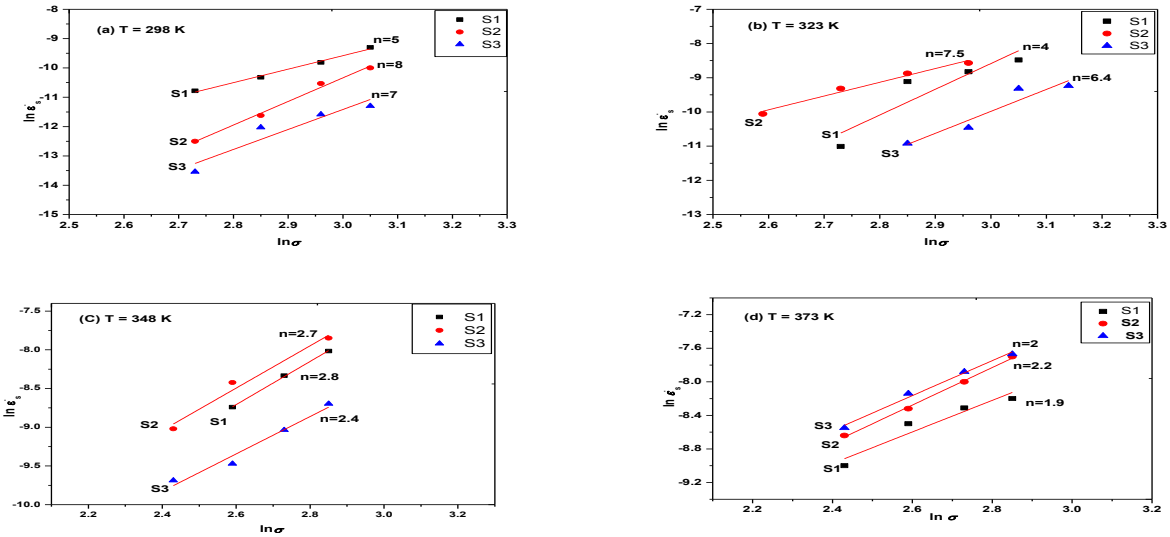

Figure 3(a, b, c, d): Linear relationships between (ln$\dot{\varepsilon}_s$ and lnσ) at different working temperatures

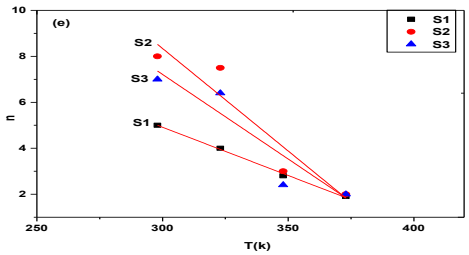

Figure 3(e): Relationships between (n) and T

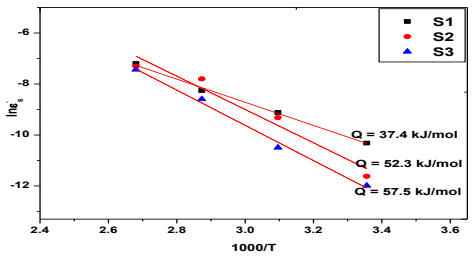

Figure 4: Linear relationships between (ln$\dot{\varepsilon}_s$ and 1/T)

Table 1: The creep characteristics (n&Q)

Alloy	N	Q (KJ/mol.)	T(K)
Sn-3.5wt.% Ag	5.0	37.4	298
	4.0		323
	2.8		348
	1.9		373
Sn-3.5wt.%Ag-0.27wt.%Ti	8.0	52.3	298
	7.5		323
	2.7		348
	2.2		373
Sn-3.5wt.%Ag-0.27wt.%Cd	7.0	57.5	298
	6.4		323
	2.4		348
	2.0		373

2.3 X-Ray Diffraction

The X-ray diffraction patterns obtained for the solidified original solder alloys (S1, S2, S3) are illustrated in Figure 5(a), only large peaks intensity of (β-Sn) rich phase and small peaks of (Ag_3Sn-IMC) phases have been detected through the eutectic (Sn-3.5Ag) based alloy. Meanwhile, new diffraction peaks of (CdSn1.9-IMC) were detected along with (β-Sn) and (Ag_3Sn) phases in the third sample (S3). The formation of the IMCs (Ag_3Sn) and (CdSn1.9) have been recognized to reinforce solder alloy and decrease the (β-Sn) grain size. are presented in Figure 5(b).

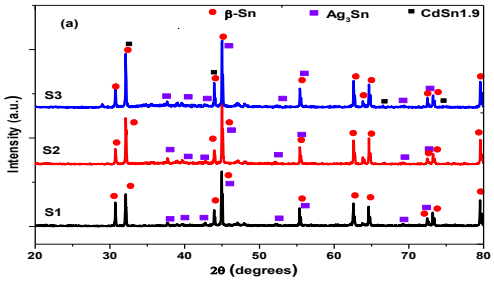

Figure 5(a): X-ray diffraction patterns for the solidified original solder alloys (S1, S2, S3)

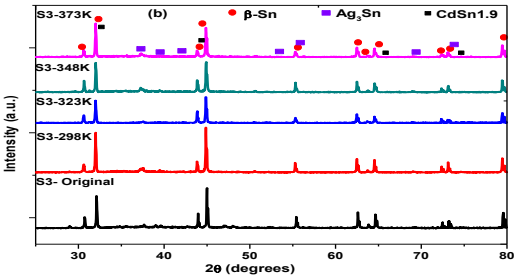

Figure 5(b): X-ray diffraction for S3 alloy at different working temperatures

The lattice parameters (a,c) for the three un-deformed original alloys (S1, S2, S3) are nearly the same with a slight decrease at the third decimal point as shown in Table 2. Figure 6(a,b) shows the relation between lattice parameters (a,c) and working temperatures (298, 323, 348 and 373K) of the crept alloy (S3) under constant applied stress (17.27MPa). The lattice parameter (a) was found to be increased in comparison with the ASTM card of (β-Sn) while the lattice parameter (c) decreased. The axial ratio (c/a) and the residual internal strains ($\Delta a/a_o$), ($\Delta c/c_o$) are illustrated in Figure 6(c,d,e) respectively. The intensities of the crystallographic planes [(211) & (411)], [(112) & (312)], are illustrated in Figure 7 (a,b).

The apparent crystallite size (L) normal to main reflection (211) plane after resolution of $K\alpha_1$ & $K\alpha_2$ intensities was calculated from half maximum full width (HMFW-B) according to Sherrer equation [30,31].

$$L = K\lambda / B\cos\theta \quad (3)$$

Where K is the Sherrer parameter equal to (0.9) for (HMFW).

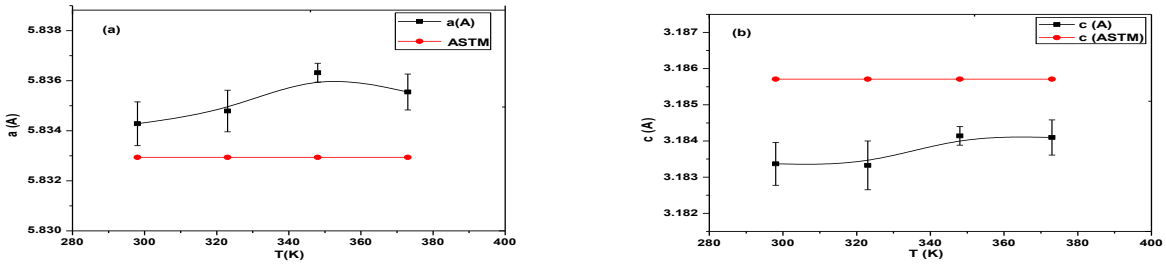

Figure 6(a, b): The lattice parameters (a, c) for S3 alloy deformed at (σ=17.27MPa) as a function of working temperatures

Table 2: The lattice parameters (a, c) for the three original un-deformed alloys (S1, S2, S3)

Parameter	S1	S2	S3
a	5.835939 ±0.000862	5.834366 ±0.00057	5.832941 ±0.000834
c	3.184295 ±0.000584	3.181942 ±0.000386	3.182765 ±0.000565

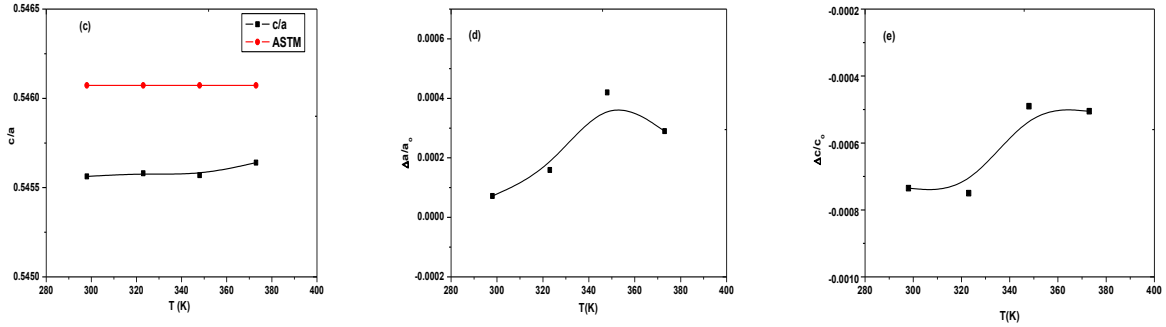

Figure 6(c, d, e): The axial ratio (c/a), the residual internal strains ($\Delta a/a_o$, $\Delta c/c_o$) as a function of working temperatures

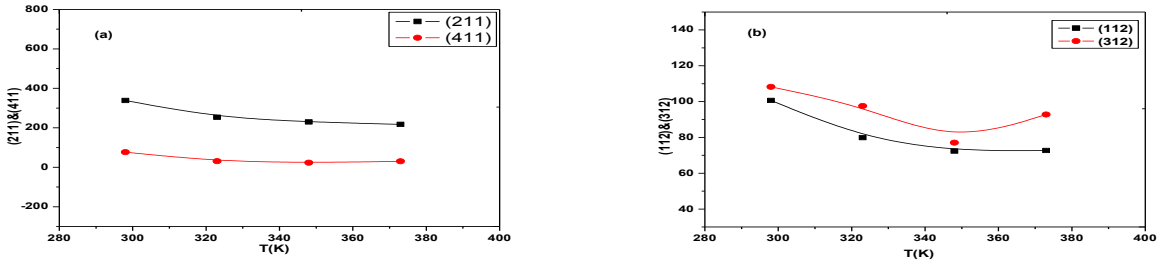

Figure 7(a, b): The intensities of crystallographic planes [(211)&(411)], [(112)&(312)] as a function of working temperatures

Figure 7(c) shows the resolution of $K\alpha_1$ and $K\alpha_2$ for (211) plane of S1 alloy as an example The calculated crystallite size values for the three original un-deformed (S1, S2, S3) samples of $K\alpha_1$ for (211) plane were found to be increased from (61.4-132.3) with the addition of (Ti or Cd) [Table 3]. The crystallite size of the deformed S3 alloy (crept at 17.27MPa) decreased from (115-78.9nm) by the effect of working temperature as shown in [Table 4 & Figure 7(d)] which means that there is a certain modification in this alloy.

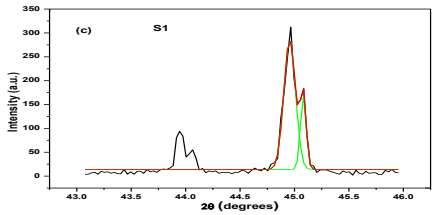

Figure 7(c): Resolution of $K\alpha_1$, $K\alpha_2$ for (211) plane of un-deformed S1 solder alloy

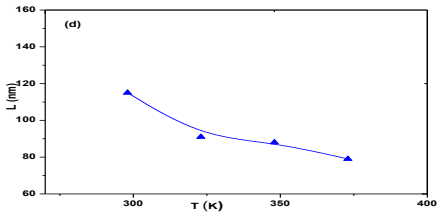

Figure 7(d): The crystallite size of the deformed S3 alloy as a function of working temperatures

Table (3): The crystallite size of (211) plane for the three original un-deformed alloys.

Samples	Crystallite size [FWHM (nm)] of (211) reflection of original alloys (S1, S2, S3)
S1	61.4
S2	104
S3	132.3

Table (4): The crystallite size of (211) plane for the deformed S3 alloy

Temperature (k)	Crystallite size [L(nm)] of (211) reflection for S3 heat treated and deformed under (σ=17.27MPa)
298	115
323	91.4
348	87.7
373	78.9

2.4 Thermal Properties

A promising solder alloys should have a lower melting temperature and a narrow pastry temperature zone which is very important for electronic applications [32-35]. A typical DTA profile of (S1, S2, S3) alloys upon heating in DTA instrument at a scanning rate of (10°C/min)is represented in Figure 8 and tabulated in Table 5.

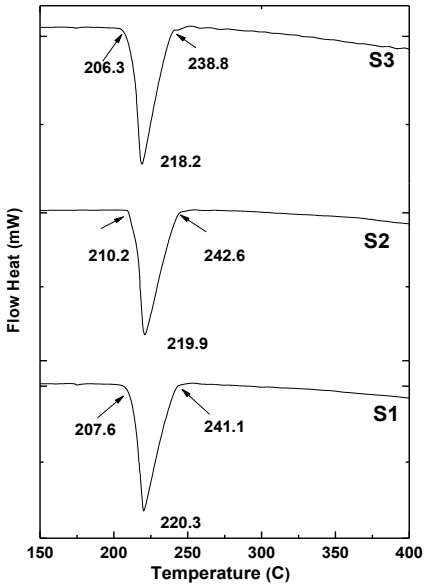

Figure 8: DTA profile of S1, S2, S3 alloys

Table 5: Thermal characteristics of the investigated solders (S1, S2, S3)

Alloy	T_{onset}(°C)	T_{end}(°C)	Pastry rang (°C)	Melting temperature (°C)
S1	207.6	241.1	33.5	220.3
S2	210.2	242.6	32.4	219.9
S3	206.3	238.8	32.5	218.2

It is clear that the alloys are characterized by end thermal peaks at (220.3, 219.9 and 218.2℃) corresponding to melting temperatures (T_m) for the binary (S1) and ternary (S2&S3) alloys. It was found that T_m as well as the pastry range (T_{end} - T_{onset}) are decreased with the addition (Ti or Cd) elements, which are in the range of the published values.

2.5 Scanning Electron Microscope

The microstructures of the un-deformed (S1, S2, S3) at room temperature are shown in Figure 9(a,b,c). The eutectic composition predicts a microstructure of mixture of Ag_3Sn (IMC) and Sn–rich phase β-Sn.

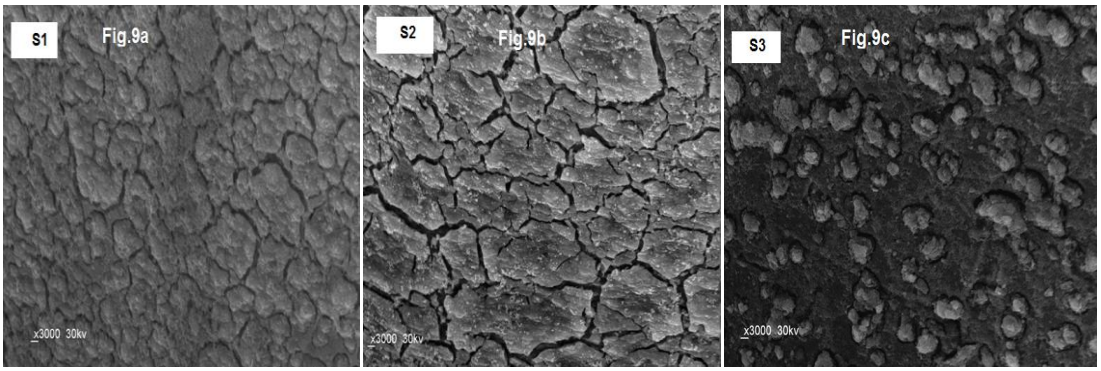

Figure 9(a, b, c): Scanning electron microscope of un-deformed S1, S2, S3 alloys at room temperature

The three alloys show fine precipitates dispersed within the β-Sn matrix which is identified from the X-ray diffraction as Ag_3Sn (IMC). The grain boundaries became thicker by the addition of (Ti) Figure 9(b). The addition of (Cd) leads to a refinement of β-Sn grains and makes some agglomeration in some areas as shown in Figure 9(c), these agglomerations increase the density of pinning centers and decreasing the dislocation mobility which makes enhancement of the strength of (S3) alloy.

3 CONCLUSIONS

In the present work, the effect of (Ti) or (Cd) element addition to Sn-3.5Ag solder alloy on the mechanical properties, microstructure and thermal analysis is examined. The results are summarized as follows:

1. Creep strength of the investigated solder alloys decreases by rising working temperatures.
2. A significant improvement in the creep resistance is achieved by (Ti) or (Cd) additions to the binary Sn-3.5Ag solder alloy.
3. The stress exponent (n) shows significant temperature dependence.
4. The presence of the third phase (Ti or Cd content) in Sn-3.5wt.%Ag alloy seems to play a significant role for reducing the melting temperature (2℃), which is technologically important for industrial development of Sn-3.5wt%Ag solder alloy.
5. In terms of the creep behavior, it was found that (S3) alloy has high creep resistance due to the fine dispersion of IMCs (Ag_3Sn and CdSn1.9). Meanwhile the (S2) alloy shows lower creep resistance than that of (S3).
6. For all the three investigated alloys, creep is dominant by pipe diffusion-controlled climb according to the obtained stress exponents and activation energies.
7. The lattice parameter (a) for (S3) alloy was found to increase in comparison with ASTM card of (β-Sn) while the lattice parameter (c) decreased. The axial ratio (c/a), the residual strains [($\Delta a/a_\circ$), ($\Delta c/c_\circ$)] and the peak height intensities (I_{hkl}) of some crystallographic planes were found in agreement with DTA & mechanical response of alloy samples. The crystallite size of (211) reflection plane at (FWHM) decreases with the working temperature.
8. The effect of the addition of each of (Ti) and (Cd) appears to refine & stabilize grain size.
9. The structural changes reflect themselves on the mechanical & physical properties of the alloy is evident while the shape & size of the grains have changed by (Cd) addition, and the boundaries become thicker by (Ti) addition.

REFERENCES

1. Ph.D. Thesis by Reda Afify Ismail, "Structural, Mechanical and Electrical Properties of Some Binary Alloys", Ain Shams Univ. (2002).
2. G.S. Al-Genainy, M.R. Nagy, *B.A. Khalifa*, R Afify, "Creep and Structural Parameters near the transformation temperature of Sn-1wt. % Pb alloy", Egyp. J. Phys. 25, 1, (2002), 57-70.
3. *B.A. Khalifa*, M.R. Nagy and R. Afify, "Effect of transformation temperatures on the electrical resistivity and structural properties of Sn-1wt. % Pb alloy using electron diffraction technique", AMSE periodical Modelling, (A), 77, (2004), 37-43.
4. K.Kawashima, T.Ito and M.Sakuragi, "Strain-rate and temperature-dependent stress-strain curves of Sn-Pb eutectic alloy", J. Matter. Sci., 27, (1992), 6387-6390.
5. HR. Kotadia, O. Mokhtari, MP. Clode, MA. Green, SH. Mannan, "Intermetallic compound growth suppression at high temperature in SAC solders with Zn addition on Cu and Ni-P substrates", J. Alloy Compd. 511 (2012) 176-188.
6. SY. Chang, CC. Jain, TH. Chuang, LP. Feng, LC. Tsao, "Effect of addition of TiO_2 nanoparticles on the microstructure, microhardness and interfacial reactions of Sn3.5AgXCu solder", Mater. Des. 32 (2011) 4720-4727.
7. ASM International, Electronic Material Handbook, 1 Materials Park, OH, (1989) 965-966.
8. E.P. Wood, K.L. Nimmo, "In search of new lead-free electronic solders", J. Electron. Mater. 23 (8) (1994) 709-713.
9. C.L. Chuang, L.C. Tsao, H.K. Lin, L.P. Feng, "Effects of small amount of Ti element additions on microstructure and property of Sn3.5Ag0.5Cu solder", Materials Science & Engineering A 558 (2012) 478-484.
10. AA. El-Daly, A. Fawzy, AZ. Mohamed and AM. El-Taher, "Micorstructrural evolution and tensile properties of Sn-5Sb solder alloy containing small amount of Ag and Cu", J. Alloy Compd. 509 (2011) 4574-4582.
11. A.Yassin, E.Gomaa, "The of microstructure and creep properties of Cu-doped Sn-4wt%Ag and Sn-9wt%Zn lead free solders with annealing temperature", Physics Journal ,1, (2015), 163- 172.
12. M.L. Hung, and L. Wang, "Effects of Cu, Bi and In on microstructure & tensile properties of Sn-Ag-X(Cu, Bi, In solders", Metall. Matter. Trans. A 36 (2005) 1439-1446.
13. L.P.Lehman, S.N. Athavale, T.Z. Fullem, A.C. Gianmis, R.K. Kinyanjui, M.Lowenstein, K. Mather, R. Patel, D. Raw, J. Wang, X. Xing, L. Zavalij, P. Borgesen and E. J. Cotts, " Growth of Sn and intermetallic compounds in Sn-Ag-Cu solder", J. Electron. Mat's, 33(12) (2004) 1429-1439.
14. S.K. Kang, W.K. Choi, D.Y. Shih, D.W. Henderson, T. Gosselin, A. Sarkhel, C. Goldsmith, K.J. Puttlitz, "Ag3Sn plate formation in the solidification of near ternary eutectic Sn-Ag-Cu alloys", J. the minerals, metals and materials (JOM) 55 (2003) 61- 65.
15. K.S. Kim, S.H. Huh, K. Suganuma, "Effects of forth alloying additive on microstructurs and tensile properties of Sn-Ag-Cu alloy and joints with Cu", Microelectron. Reliab. 43 (2003) 259-267.
16. M. Wang, J. Wang, H. Feng, W.Ke, "Effect of Ag_3Sn inetermetallic compounds on corrosion of Sn-3.0Ag-0.5Cu solder under high temperature & high humidity condition", Corros, Sci. 63 (2012) 20-28.
17. M.L. Huang, L. Wang and C.M.L. Wu, "Creep behavior of eutectic Sn-Ag lead-free solder alloy", J. of Mater. Research 17 Issue 11 (2002) 2897-2903.
18. F. Lin, W.Bi, G. Ju, W.Wang, X.Wei, "Evolution of Ag_3Sn at Sn-3.0Ag-0.3Cu-0.05Cr/Cu joint interfaces during thermal aging", J. Alloy Compd., 509 (2011) 6666-6672.
19. A. Abtew, G. Selvaduray, "Lead-free solders in microelectronics", Mater, Sci. Eng. Rep. 27(5-6) (2000) 95-141.
20. I.E. Anderson, J.C. Foley, B.A. Cook, J. Harringa, R.L. Terpstra, O.Unal, "Alloying effects in near-eutectic Sn-Ag-Cu solder alloys for improved microstrctural stability", J. electron. Mater. 30 (9) (2001) 1050-1059.

21. M. McCormack, S. Jin, G.W. Kammlott, H.S. Chen, "New Pb-free solder alloy with superior mechanical properties", Appl. Phys. Lett.63 (1) (1993) 15-17.
22. A.Z. Miric and A. Grusd, "Lead-free alloys", Soldering Surf. Mount Technol. 10 (1) (1998) 19-25.
23. ICdA International Cadmium Association.[http://www.cadmium.org/cadmium-applications/cadmium-in-alloys]
24. Mustafa Kamal, Abu Bakr El-Bediwi, and Tarek El-Ashram, "The effect of rapid solidification on the structure, decomposition behavior, electrical and mechanical properties of the Sn-Cd binary alloys", J. of Mater Science: Materials in Electronics 15 (2004) 211-217.
25. A.E. Hammad, "Investigation of microstructure and mechanical properties of novel Sn-0.5Ag-0.7Cu solders containing small amount of Ni", Materials and design 50 (2013) 108-116.
26. A.A. El-Daly, A.Z. Mohamed, A. Fawzy and A.M. El-Taher, "Creep behavior of near peritectic Sn-5Sb solders containing small amount of Ag and Cu", Mater. Sci. Eng. A 528 (2011) 1055-1062.
27. A.A. El-Daly, A.E. Hammad "Enhancement of creep resistance and thermal behavior of eutectic Sn-Cu lead- free solder alloy by Ag and In-additions", Materials and Design 40 (2012) 292-298.
28. A.A. El-Daly, "Tensile properties of Pb-Sn bearing alloy containing small amount of Sb", Phys. Stat. Sol. A 201 (2004) 2035-2041.
29. D. Witkin, "Creep behavior of Bi- containing lead free solder alloy", J. Electron Mater .41 (2) (2012) 190-203.
30. M.T. Nawar, B.A. khalifa, G.S. Al-Ganainy, and A.W. Shalaby, "Crystallinity, crystallite size and some physical properties of two fiber maturity levels in some Egyptian cotton cultivars", Egyp. J. Sol.18,(1), (1995) 61-73.
31. N. Barakat, B.A. Khalifa, F. Sharaf and A. El-Bahy, "X-ray diffraction studies of ɣ- irradiated Nylon 6 (Polycapramide) fibers", Egyp. J. Phys. 15 (2), (1984) 237-246.
32. P.Babaghorbani, S.M.L. Nai, M. Gupta, "Development of lead free Sn-3.5Ag/SnO_2 nanocomposite solder" Journal of Material Science, Mater Electron 20 (2009) 571-576.
33. A .Haseeb, M.M. Arafat, and M.R. Johan, "Stability of Molybdenum nanoparticles Sn-3.8Ag-0.7Cu solder during multiple reflow and their influence on interfacial intermetallic compounds", Journal of Materials Characterization 64 (2012) 27-35.
34. A.A .El-Daly, A.E. Hammad, G.S. Al-Ganainy, and M. Ragab, "Properties enhancement of low Ag-content Sn-Ag-Cu lead-free solders containing small amount of Zn", Journal of Alloys and Compounds, 614 (2014) 20-28.
35. A.A. El-Daly, A.E. Hammad, G.S. Al-Ganainy, and A.A. Ibrahiem, "Design of lead-free candidate alloys for low-temperature soldering application based on the hypoeutectic Sn-6.5Zn alloys", Materials and Design 56 (2014) 594-603.

DOI : 10.24297/jap.v13i8.6357